

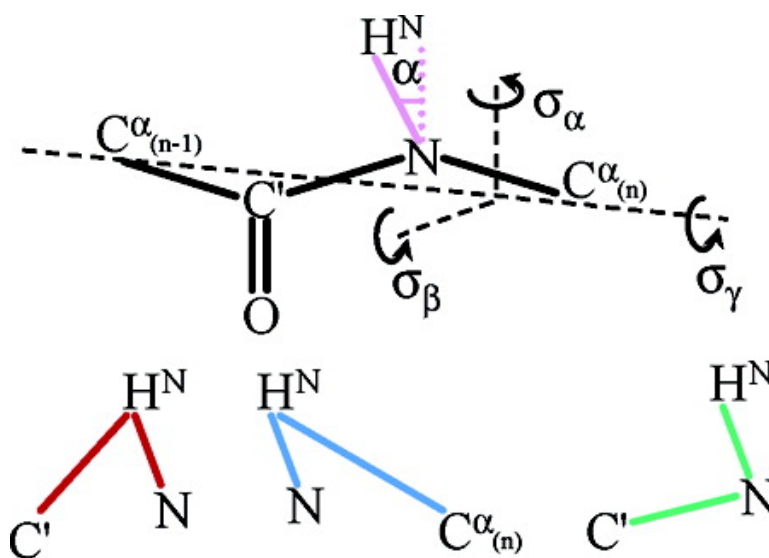
Article

## Anisotropic Local Motions and Location of Amide Protons in Proteins

Dimitri Bytchenkoff, Philippe Pelupessy, and Geoffrey Bodenhausen

*J. Am. Chem. Soc.*, **2005**, 127 (14), 5180-5185 • DOI: 10.1021/ja043575v • Publication Date (Web): 17 March 2005

Downloaded from <http://pubs.acs.org> on March 25, 2009



### More About This Article

Additional resources and features associated with this article are available within the HTML version:

- Supporting Information
- Access to high resolution figures
- Links to articles and content related to this article
- Copyright permission to reproduce figures and/or text from this article

[View the Full Text HTML](#)



**ACS Publications**  
 High quality. High impact.

## Anisotropic Local Motions and Location of Amide Protons in Proteins

Dimitri Bytchenkoff,<sup>†,‡</sup> Philippe Pelupessy,<sup>†,‡</sup> and Geoffrey Bodenhausen<sup>\*,†,‡</sup>

*Contribution from the Institut des Sciences et Ingénierie Chimiques, Ecole Polytechnique Fédérale de Lausanne, BCH, 1015 Lausanne, Switzerland, and Département de Chimie, associé au CNRS, Ecole Normale Supérieure, 24 rue Lhomond, 75231 Paris Cedex 05, France*

Received October 22, 2004; E-mail: Geoffrey.Bodenhausen@ens.fr

**Abstract:** A new method has been developed to obtain dynamic and structural information about peptide planes in proteins by a combination of measurements of weak short-range cross-correlation rates  $R(\text{H}^{\text{N}}/\text{NC}')$  that are due to concerted fluctuations of the  $\text{H}^{\text{N}}-\text{N}$  and  $\text{N}-\text{C}'$  dipole-dipole interactions and stronger long-range cross-correlation rates  $R(\text{C}'\text{H}^{\text{N}}/\text{H}^{\text{N}})$  and  $R(\text{NH}^{\text{N}}/\text{H}^{\text{N}}\text{C}^{\alpha})$ . The rates were interpreted using the axially symmetric Gaussian axial fluctuation model (GAF). The oscillation amplitudes as well as the positions of  $\text{H}^{\text{N}}$  atoms with respect to peptide planes in ubiquitin were determined. Most  $\text{N}-\text{H}^{\text{N}}$  bonds were found not to lie exactly along the bisector of the  $\text{N}-\text{C}'$  and  $\text{N}-\text{C}^{\alpha}$  bonds but to be slightly tilted toward the carbon-terminal side of the peptide.

### Introduction

The internal mobility along the backbone of proteins is usually probed by measuring the auto-correlated relaxation rates ( $R_1 = 1/T_1$ ,  $R_2 = 1/T_2$ ) and heteronuclear NOEs of the amide nitrogen nuclei.<sup>1</sup> Although these kinds of measurements give an adequate qualitative indication about the amplitude of fast internal motions, they do not give any information about their nature. A number of more sophisticated studies have been published which attempt to characterize anisotropic internal motions of the peptide plane, often giving contradictory results. Ernst and co-workers<sup>2</sup> measured autocorrelated relaxation rates of both carbonyl carbon and amide nitrogen nuclei at different static magnetic fields  $B_0$  and interpreted the rates in terms of their three-dimensional Gaussian axial fluctuations (3D-GAF) model. A number of works focused on the study of different cross-correlated relaxation rates.<sup>3,4</sup> These investigations seemed to indicate that the internal motions of nonterminal amino acids are dominated by oscillations of the peptide planes about the  $\text{C}^{\alpha}(\text{n}-1)-\text{C}^{\alpha}(\text{n})$  axes. The main disadvantage of these methods is that the interpretation of the experimental rates critically depends on the exact knowledge of the orientation and amplitude of the chemical shift anisotropy (CSA) tensors of carbonyl carbon  $\text{C}'$  and amide nitrogen  $\text{N}$  atoms. Zuiderweg and co-workers<sup>5</sup> have recently investigated the temperature dependence of the order parameter  $S^2(\text{N}-\text{H}^{\text{N}})$  and the cross-correlated

relaxation rate due to the correlated fluctuations of the  $\text{C}'$  CSA and  $\text{C}'-\text{C}^{\alpha}$  dipolar interactions and concluded that the internal motions were *not* primarily governed by fluctuations about the  $\text{C}^{\alpha}(\text{n}-1)-\text{C}^{\alpha}(\text{n})$  axis. Several studies made use of residual dipolar couplings which are not averaged to zero when a protein is dissolved in anisotropic media.<sup>6-8</sup> By measuring the residual dipolar couplings in proteins in at least five independent orientations one can extract information about the internal motions. The residual dipolar couplings are sensitive to motions as slow as a few kHz. By comparing experimental results with molecular dynamic simulations, Griesinger and co-workers<sup>6</sup> concluded that fast internal motions, i.e., motions faster than the correlation time  $\tau_c$ , were mainly axially symmetrical around the  $\text{N}-\text{H}^{\text{N}}$  bond, while the slower ones were highly anisotropic. Bax and co-workers<sup>8</sup> concluded that the residual dipolar couplings are very sensitive to the average positions of the  $\text{N}-\text{H}^{\text{N}}$  vectors with respect to the amide plane. Apart from a few residues, they obtained an excellent fit by assuming a common amide order parameter for most peptide planes of the entire protein. Nevertheless they could not exclude that the amplitudes of fluctuations about the  $\text{C}^{\alpha}(\text{n}-1)-\text{C}^{\alpha}(\text{n})$  axis were up to  $12^\circ$  larger than those around perpendicular axes. Bernadó and Blackledge<sup>9</sup> found a significant improvement in the fit of the alignment tensors of several proteins by using a common 1D GAF model for all peptide planes instead of a static model.

Much has been written and speculated about the precise positions of hydrogen nuclei in a wide range of biomolecular systems, as their coordinates are essentially invisible in X-ray diffraction studies. Neutron diffraction studies<sup>10</sup> can provide

<sup>†</sup> Ecole Polytechnique Fédérale, Lausanne, Switzerland.

<sup>‡</sup> Ecole Normale Supérieure, Paris, France.

- (1) Peng, J. W.; Wagner, G. *J. Magn. Reson.* **1982**, *98*, 308–332.
- (2) Lienin, S. F.; Bremi, T.; Brutscher, B.; Brüschweiler, R.; Ernst, R. R. *J. Am. Chem. Soc.* **1998**, *120*, 9870–9879.
- (3) Brutscher, B.; Skrynnikov, N. R.; Bremi, T.; Brüschweiler, R.; Ernst, R. R. *J. Magn. Reson.* **1998**, *130*, 346–351.
- (4) Carlomagno, T.; Maurer, M.; Hennig, M.; Griesinger, C. *J. Am. Chem. Soc.* **1998**, *122*, 5105–5113.
- (5) Wang, T. Z.; Cai, S.; Zuiderweg, E. R. P. *J. Am. Chem. Soc.* **2003**, *125*, 8639–8643.

- (6) Peti, W.; Meiler, J.; Brüschweiler, R.; Griesinger, C. *J. Am. Chem. Soc.* **2002**, *124*, 5822–5833.
- (7) Tolman, J. R. *J. Am. Chem. Soc.* **2002**, *124*, 12020–12030.
- (8) Ulmer, T. S.; Ramirez, B. E.; Delaglio, F.; Bax, A. *J. Am. Chem. Soc.* **2003**, *125*, 9179–9191.
- (9) Bernadó, P.; Blackledge, M. *J. Am. Chem. Soc.* **2004**, *126*, 4907–4920.

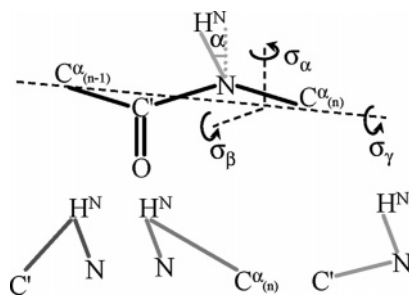


**Figure 1.** Fragment of a peptide plane showing the angle  $\alpha$  that describes how much the N–H<sup>N</sup> bond deviates from the bisector of the angle subtended by the N–C' and N–C <sup>$\alpha$</sup>  bonds. The pairs of dipole–dipole interactions C'–H<sup>N</sup> and H<sup>N</sup>–N, N–H<sup>N</sup> and H<sup>N</sup>–C <sup>$\alpha$</sup> , as well as H<sup>N</sup>–N and N–C' are indicated in red, blue, and green, respectively. The cross-correlated relaxation processes that were measured in this work are due to correlated fluctuations of these interactions.

useful information, but relatively few biomolecules have been investigated in detail so far. Furthermore the precision of these studies leaves much to be desired. Solid-state NMR methods<sup>11,12</sup> offer unique perspectives to locate hydrogen nuclei, since dipolar interactions provide an accurate measure of distances, while correlations with anisotropic chemical shifts provide a measure of relative orientations. In liquid-state NMR, scalar<sup>13</sup> and more recently residual dipolar couplings<sup>8</sup> have been used to locate amide protons with respect to peptide planes. The detailed study of cross-correlated relaxation effects in solution-state NMR has made such progress in recent years that accurate information can now be extracted not only about distances but also about angles between various bonds or, more generally, between various short- or long-range dipolar interactions.<sup>14,15</sup>

In this work we are concerned with obtaining a clearer vision of the nature of anisotropic internal motions by measuring complementary cross-correlation rates. This approach allows us to obtain dynamical and structural information. Our method also enables us to determine how much the N–H<sup>N</sup> bond deviates from the bisector of C'–N and N–C <sup>$\alpha$</sup>  bonds. We rely exclusively on dipolar interactions and, by doing so, avoid uncertainties related to the principal components and orientation of CSA tensors.

## Theory

Three different DD/DD cross-correlation rates are indicated on the peptide plane in Figure 1: in red  $R(C'H^N/H^N)$ , in blue  $R(NH^N/H^NC^{\alpha})$ , and in green  $R(H^N/NC')$ . C <sup>$\alpha$</sup>  belongs to the same residue, while C' belongs to the previous amino acid in the sequence. The covalent angles and distances of the heavy atoms, as determined from very high-resolution X-ray structures, show relatively little variation.<sup>16</sup> Usually, it is assumed that the N–H<sup>N</sup> vector lies in the peptide plane defined by the O, C', and N atoms and bisects the C'NC <sup>$\alpha$</sup>  angle. We define the angle

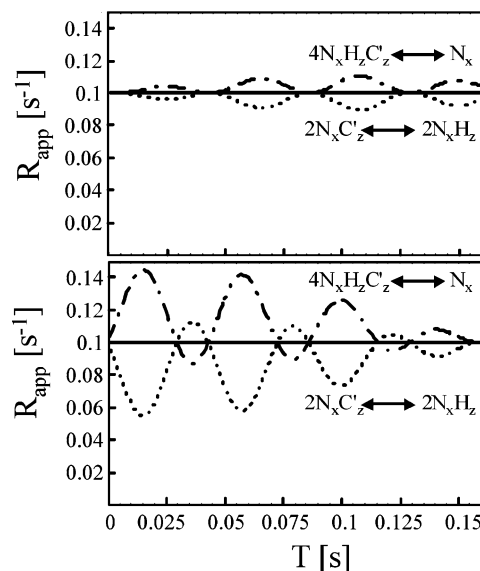


**Figure 2.** (Top) Simulations based on calculations in Liouville space of deviations in rates caused by violations of the secular approximation during the relaxation period  $T$  in the sequence of Figure S1c. The scalar couplings were assumed to be  $^1J(H^N) = -93$  Hz,  $^1J(NC') = 15$  Hz and  $^2J(H^NC') = 3$  Hz. The longitudinal relaxation rates were assumed to be  $R_1(H^N) = 6$  s<sup>-1</sup> and  $R_1(C') = 1$  s<sup>-1</sup>. The autorelaxation rates of the different coherences were assumed to be equal to the sum of the autorelaxation rates of the different components of the coherences, e.g.,  $R(4N_x H_z C'_z) = R_2(N) + R_1(H^N) + R_1(C')$ . (Top) although the “true” value of  $R(H^N/NC')$  was set to 0.1 s<sup>-1</sup> in the simulations, the apparent cross-correlation rate  $R_{app}(H^N/NC')$  obtained from eq 5 ranges between 0.09 and 0.11 s<sup>-1</sup>. By contrast, eq 6 gives an ideal answer. (Bottom) Calculated errors caused by violations of the secular approximation in combination with pulse imperfections. All proton and carbon refocusing and inversion pulses in the  $T$  interval of Figure S1c were assumed to be 185.4° rather than 180° (+3%). The deviation of the apparent rate  $R(H^N/NC')$  from its “true” value can be as large as 40%. Again, eq 6 gives the true value.

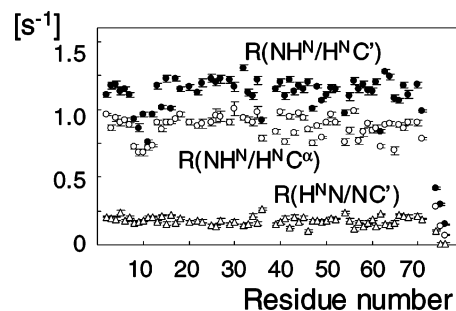


**Figure 3.** Three experimental cross-correlation rates (●)  $R(C'H^N/H^N)$ , (○)  $R(NH^N/H^NC^{\alpha})$ , and (Δ)  $R(H^N/NC')$  as listed in Table S1, measured using the schemes of Figure S1a, b, and c, for most peptide planes of <sup>15</sup>N- and <sup>13</sup>C-labeled ubiquitin at 300 K, 600 MHz, 1.5 mM in 90% H<sub>2</sub>O and 10% D<sub>2</sub>O at pH = 4.5.

$\alpha$  as the deviation from the latter condition. The three cross-correlation rates depend on the angles between the different interactions and on the amplitude and anisotropy of the internal motion. The only unknown structural quantity is the  $\alpha$ -angle. Note that it is also possible that the N–H<sup>N</sup> vector is tilted slightly away from the peptide plane owing to the “pyramidalisation” of the nitrogen bond. However, such a deviation would only affect the three rates significantly for very large tilt angles. A tilt of 10° changes the different cross-correlated relaxation rates by less than 0.01 s<sup>-1</sup>.

The single quantum cross-correlation rate due to correlated fluctuations of two dipole–dipole interactions can be written

- (10) Fong, S.; Ramakrishnan, V.; Schoenborn, B. P. *Proc. Natl. Acad. Sci.* **2000**, *97*, 3872–3875.
- (11) Hohwy, M.; Jaroniec, C. P.; Reif, B.; Rienstra, C. M.; Griffin, R. G. *J. Am. Chem. Soc.* **2000**, *122*, 3218–3219.
- (12) Zhao, X.; Sudmeijer, J. L.; Bachovchin, W. W.; Levitt, M. H. *J. Am. Chem. Soc.* **2001**, *123*, 11097–11098. Zhao, X.; Hoffbauer, W.; auf der Gunne, J. S.; Levitt, M. H. *Solid State Nucl. Magn. Reson.* **2004**, *26*, 57–64.
- (13) Hu, J. S.; Bax, A. *J. Am. Chem. Soc.* **1997**, *119*, 6360–6368.
- (14) Reif, B.; Hennig, M.; Griesinger, C. *Science* **1997**, *276*, 1230–1233.
- (15) Kumar, A.; Grace, R. C. R.; Madhu, P. K. *Prog. Nucl. Magn. Reson. Spectrosc.* **2000**, *37*, 191–319. Brutscher, B. *Concept Magn. Reson.* **2000**, *12*, 207–229.
- (16) Engh, R. A.; Huber, R. *Acta Crystallogr., Sect. A* **1991**, *37*, 392–400.

as follows<sup>17</sup>

$$R(\text{AX}/\text{XB}) = \left(\frac{\mu_0 \hbar}{4\pi}\right)^2 \frac{\gamma_A \gamma_X^2 \gamma_B}{r_{\text{AX}}^3 r_{\text{XB}}^3} [4J_{\text{AX}/\text{XB}}(0) + 3J_{\text{AX}/\text{XB}}(\omega_X)] \quad (1)$$

where  $r_{\text{AX}}$  and  $r_{\text{XB}}$  stand for the distances between corresponding atoms, and the other symbols have the usual meanings. Provided that overall tumbling is isotropic, which is a reasonable assumption for many proteins, the cross-correlated spectral density  $J_{\text{AX}/\text{XB}}(\omega_X)$  can be expressed as<sup>18</sup>

$$J_{\text{AX}/\text{XB}}(\omega_X) = S_{\text{AX}/\text{XB}}^2 \frac{2\tau_c}{1 + (\omega_X \tau_c)^2} + \left[ \frac{(3 \cos^2 \Theta_{\text{AX}/\text{XB}} - 1)}{2} - S_{\text{AX}/\text{XB}}^2 \right] \frac{2\tau_{\text{AX}/\text{XB}}^{\text{eff}}}{1 + (\omega_X \tau_{\text{AX}/\text{XB}}^{\text{eff}})^2} \quad (2)$$

where the order parameter  $S_{\text{AX}/\text{XB}}^2$  expresses how the effective dipolar interactions AX and XB are scaled by fast internal motions,  $\Theta_{\text{AX}/\text{XB}}$  is the angle between the two dipolar interactions, and  $1/\tau_{\text{AX}/\text{XB}}^{\text{eff}} = 1/\tau_c + 1/\tau_{\text{int}}$ , where  $\tau_c$  is the correlation time for overall tumbling and  $\tau_{\text{int}}$  is the characteristic correlation time for the internal motion.

In the absence of internal motion the order parameter reduces to

$$S_{\text{AX}/\text{XB}}^2 = \frac{(3 \cos^2 \Theta_{\text{AX}/\text{XB}} - 1)}{2} \quad (3)$$

The motions that drive the auto- and cross-correlated relaxation of single- and multiple-quantum coherences involving the peptide backbone atoms  $^{15}\text{N}$ ,  $^{13}\text{C}'$ ,  $^{13}\text{C}^\alpha$ , and  $^1\text{H}^{\text{N}}$  are expected to be affected by anisotropic oscillations of the peptide planes, which are assumed to be rigid.<sup>2</sup> The generalized order parameter  $S_{\text{AX}/\text{XB}}^2$  can be interpreted in terms of three independent Gaussian axial fluctuations (3D GAF model) about three orthogonal axes:<sup>19,20</sup>

$$S_{\text{AX}/\text{XB}}^2 = \frac{4\pi}{5} \sum_{l,k,k',m,m'=-2}^2 (-1)^{k-k'} \exp \left\{ -\frac{\sigma_\alpha^2 (k^2 + k'^2)}{2} - \frac{\sigma_\beta^2 l^2 - \frac{\sigma_\gamma^2 (m^2 + m'^2)}{2}}{2} \right\} \times$$

$$d_{kl}^{2(\frac{\pi}{2})} d_{kl}^{2(\frac{\pi}{2})} d_{mk}^{2(\frac{\pi}{2})} d_{m'k'}^{2(\frac{\pi}{2})} Y_{2m}(\Theta_{\text{AX}}, \varphi_{\text{AX}}) Y_{2m'}(\Theta_{\text{XB}}, \varphi_{\text{XB}}) \quad (4)$$

where  $d_{kl}^{2(\pi/2)}$  are reduced Wigner matrix elements and  $Y_{2m}(\Theta_{\text{AXB}}, \varphi_{\text{AX}})$  are second-order spherical harmonics.

## Methods

Three experimental schemes were developed to measure the dipole–dipole cross-correlation rates  $R(\text{C}'\text{H}^{\text{N}}/\text{H}^{\text{N}})$ ,  $R(\text{NH}^{\text{N}}/\text{H}^{\text{N}}\text{C}^\alpha)$ , and  $R(\text{H}^{\text{N}}/\text{NC}')$  using the principle of symmetrical reconversion.<sup>21</sup> The scheme

comprising the four complementary experiments I–IV of Figure S1a (Supporting Information) is designed to measure the strong, albeit long-range, effect  $R(\text{C}'\text{H}^{\text{N}}/\text{H}^{\text{N}})$ . Transverse magnetization  $H^{\text{N}}_X$  is excited at the beginning of the relaxation delay  $T$  in experiments I and II. Using the one-bond scalar couplings  $^1J(\text{H}^{\text{N}}\text{N})$  and  $^1J(\text{NC}')$ , the product operator  $4H^{\text{N}}_X N_Z C'_Z$  is created at the start of the delay  $T$  in experiments III and IV. The effects of the scalar couplings and most cross-correlation mechanisms except for the desired rate  $R(\text{C}'\text{H}^{\text{N}}/\text{H}^{\text{N}})$  are averaged to zero by applying suitable  $180^\circ$  pulses during the relaxation period  $T$ . After this delay transverse magnetization  $H^{\text{N}}_X$  is selected in experiments I and III, while doubly antiphase coherence  $4H^{\text{N}}_X N_Z C'_Z$  is selected in experiments II and IV. The experimental  $R(\text{C}'\text{H}^{\text{N}}/\text{H}^{\text{N}})$  rates were extracted from the amplitudes of the signals of the four complementary experiments:

$$R(\text{C}'\text{H}^{\text{N}}/\text{H}^{\text{N}}) = \frac{1}{T} \tanh^{-1} \left( \sqrt{\frac{\langle A \rangle_{\text{II}}(T) \langle A \rangle_{\text{III}}(T)}{\langle A \rangle_{\text{I}}(T) \langle A \rangle_{\text{IV}}(T)}} \right) \quad (5)$$

We use the same approach to measure the rate  $R(\text{NH}^{\text{N}}/\text{H}^{\text{N}}\text{C}^\alpha)$  (see Figure S1b). Cross-correlated relaxation causes an interconversion between  $H^{\text{N}}_X$  and  $4H^{\text{N}}_X N_Z C^\alpha_Z$ . To prepare these operators we use a number of INEPT-like steps.<sup>22–24</sup>

The weaker short-range cross-correlation rate  $R(\text{H}^{\text{N}}/\text{NC}')$  is more difficult to detect, since it is an order of magnitude smaller than  $R(\text{C}'\text{H}^{\text{N}}/\text{H}^{\text{N}})$ . Figure 2 shows that a simple four-step scheme analogous to Figures S1a and b would fail to eliminate the errors which arise from violations of the secular approximation and from pulse imperfections. These errors can amount to up to 45% for unfavorable relaxation delays. Therefore, we designed a new eight-step scheme (see Figure S1c) to measure the weak rate  $R(\text{H}^{\text{N}}/\text{NC}')$ . One of the four product operators  $2N_X H^{\text{N}}_Z$ ,  $2N_X C'_Z$ ,  $N_X$ , or  $4N_X H^{\text{N}}_Z C'_Z$  is excited at the beginning of the relaxation delay  $T$ . After this delay, these coherences are detected selectively in suitable experiments. Most cross-correlation effects except  $R(\text{H}^{\text{N}}/\text{NC}')$  are averaged to zero by applying  $180^\circ$  pulses during the relaxation period. The effects of the scalar couplings are also averaged out by  $180^\circ$  pulses. The experimental  $R(\text{H}^{\text{N}}/\text{NC}')$  rates were determined from the eight supplementary experiments:

$$R(\text{H}^{\text{N}}/\text{NC}') = \frac{1}{2T} \left[ \tanh^{-1} \left( \sqrt{\frac{\langle A \rangle_{\text{II}}(T) \langle A \rangle_{\text{III}}(T)}{\langle A \rangle_{\text{I}}(T) \langle A \rangle_{\text{IV}}(T)}} \right) + \tanh^{-1} \left( \sqrt{\frac{\langle A \rangle_{\text{VI}}(T) \langle A \rangle_{\text{VII}}(T)}{\langle A \rangle_{\text{V}}(T) \langle A \rangle_{\text{VIII}}(T)}} \right) \right] \quad (6)$$

To take into account the internal correlation time  $\tau_{\text{int}}$  in eq 2, the heteronuclear cross-relaxation (NOE) rates (as determined by the ratio  $\eta$  between the signal intensities of an experiment in which the protons are saturated and the signal intensities of a reference experiment in which the protons are not perturbed) and the longitudinal auto-relaxation rates  $R_1(\text{N})$  of the nitrogen nuclei have been measured.

$$\text{NOE}(\text{H} \rightarrow \text{N}) = (\eta - 1) \frac{\gamma_{\text{N}}}{\gamma_{\text{H}}} R_1(\text{N}) =$$

$$\left(\frac{\mu_0 \hbar}{4\pi}\right)^2 \frac{\gamma_{\text{H}}^2 \gamma_{\text{N}}^2}{r_{\text{NH}}^6} [12J_{\text{NH},\text{NH}}(\omega_{\text{N}} + \omega_{\text{H}}) - 2J_{\text{NH},\text{NH}}(\omega_{\text{N}} - \omega_{\text{H}})] \quad (7)$$

These rates depend only on the spectral densities near the proton Larmor frequency (which makes them very sensitive to fast internal motions) and on the orientation of the  $\text{NH}^{\text{N}}$  vectors; hence no additional geometric variables are needed.

The overall correlation time has been determined by measuring the transverse and longitudinal  $\text{N}/\text{NH}^{\text{N}}$  DD/CSA cross-correlation rates.

(17) Frueh, D. *Prog. Nucl. Magn. Reson. Spectrosc.* **2002**, *41*, 305–324.

(18) Lipari, G.; Szabo, A. *J. Am. Chem. Soc.* **1982**, *104*, 4546–4559.

(19) Bremi, T.; Büschweiler, R. *J. Am. Chem. Soc.* **1997**, *119*, 6672–6673.

(20) Brüschweiler, R.; Wright, P. E. *J. Am. Chem. Soc.* **1994**, *116*, 8426–8427.

(21) Pelupessy, P.; Espallargas, G. M.; Bodenhausen, G. *J. Magn. Reson.* **2003**, *161*, 258–264.

(22) Chiarparin, E.; Pelupessy, P.; Ghose, R.; Bodenhausen, G. *J. Am. Chem. Soc.* **2000**, *122*, 1758–1761.

(23) Permi, P. *J. Biomol. NMR* **2002**, *23*, 201–209.

(24) Brutscher, B. *J. Magn. Reson.* **2002**, *156*, 155–159.

## Anisotropic Local Motions and Location of Amide Protons in Proteins

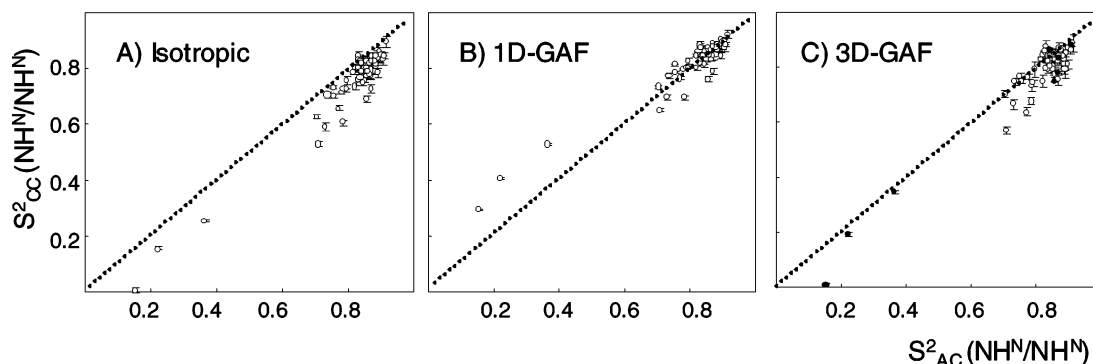


**Figure 4.** Correlations of the order parameter  $S^2_{CC}(\text{NH}^N/\text{NH}^N)$  obtained from the cross-correlation rates of Table S1 (see also Figure 3) against the order parameter  $S^2_{AC}(\text{NH}^N/\text{NH}^N)$  determined by Tjandra et al.<sup>27</sup> from autocorrelated relaxation rates using (A) a model with isotropic internal motions, (B) the 1D-GAF model, and (C) the axially symmetric 3D-GAF model.

These measurements allowed us to determine the axially symmetric rotational diffusion tensor.<sup>25</sup> The different relaxation rates have been corrected for the slight deviation from isotropic diffusion.

### Results and Discussion

The experimental schemes described in the previous section were applied to a sample of  $^2\text{H}$ -,  $^{15}\text{N}$ -, and  $^{13}\text{C}$ -labeled human ubiquitin. The experimental  $R(\text{C}'\text{H}^N/\text{H}^N)$ ,  $R(\text{NH}^N/\text{H}^N\text{C}^\alpha)$ , and  $R(\text{H}^N/\text{NC}')$  rates observed at 14 T (600 MHz for protons) are shown in Figure 3. The numerical values of the rates are presented in Table 1S of the Supporting Information. These rates depend on both local structure and internal motions.

In a first isotropic approximation (A), we assumed that for each peptide plane the local motions affect all three rates  $R(\text{C}'\text{H}^N/\text{H}^N)$ ,  $R(\text{NH}^N/\text{H}^N\text{C}^\alpha)$ , and  $R(\text{H}^N/\text{NC}')$  identically, i.e., that the rates are scaled by the same factor,  $S^2(\text{AX}/\text{XB}) \approx S^2\text{P}_2(\cos \Theta_{\text{AX}/\text{XB}})$ . Assuming that the  $\text{N}-\text{H}^N$  and  $\text{C}'-\text{H}^N$  bond lengths are equal to 1.02 and 1.33 Å, respectively, and that the angle  $\text{C}'\text{N}\text{C}^\alpha$  is equal to  $121.7^\circ$ ,<sup>24</sup> only two variables, i.e.,  $\alpha$  and  $S^2$ , determine the three cross-correlation rates. The  $S^2$  parameters determined in this manner agree reasonably well with autocorrelated order parameters  $S^2(\text{NH}^N/\text{NH}^N)$  derived previously<sup>27</sup> from  $^{15}\text{N}$  autorelaxation, although there is a systematic deviation, as can be seen in Figure 4A.

In a second approximation (B), we determined the angle  $\alpha$  and the amplitudes of the oscillations  $\sigma_\gamma$  about the  $\text{C}^\alpha(\text{n}-1)-\text{C}^\alpha(\text{n})$  axes, assuming  $\sigma_\alpha = \sigma_\beta = 0$ .<sup>1</sup> This 1D-GAF model yields three distinct order parameters  $S^2(\text{C}'\text{H}^N/\text{H}^N)$ ,  $S^2(\text{NH}^N/\text{H}^N\text{C}^\alpha)$ , and  $S^2(\text{H}^N/\text{NC}')$  corresponding to the three observed cross-correlated rates. With these two parameters, one can predict the order parameters  $S^2(\text{NH}^N/\text{NH}^N)$  corresponding to the autocorrelated relaxation rates of the  $\text{N}-\text{H}^N$  vector. The  $S^2(\text{NH}^N/\text{NH}^N)$  order parameters that were predicted in this manner no longer show any systematic deviation from the autocorrelated order parameters  $S^2(\text{NH}^N/\text{NH}^N)$  that were determined experimentally (Figure 4B), although there is still some dispersion. Interestingly, the  $\alpha$  angles calculated using the two approaches A and B have opposite signs (Figure 5A and B). Model A with a single order parameter for each residue suggests that the  $\text{N}-\text{H}^N$  bonds are

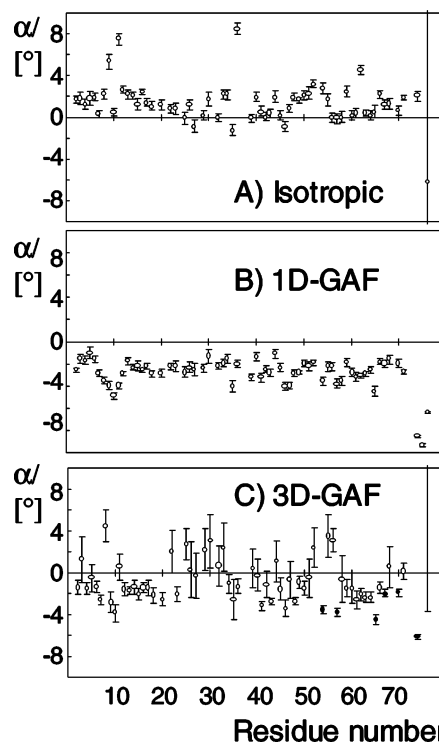


**Figure 5.** Values of the angle  $\alpha$  that describes the location of  $\text{H}^N$  (see Figure 1) obtained from three cross-correlation rates of Table S1 (see also Figure 3) using models with (A) isotropic internal motions, (B) 1D-GAF, or (C) axially symmetric 3D-GAF.

slightly tilted to the left ( $\alpha > 0$  in Figure 1), while the 1D GAF model B suggests that they are slightly tilted toward the right ( $\alpha < 0$ ). The average  $\chi^2$  value of model B diminished from 9.4 to 6.1 compared to model A.

In a third approximation, we used an axially symmetric 3D GAF model (C) where for each peptide plane three parameters  $\alpha$ ,  $\sigma_\gamma$ , and  $\sigma_\alpha = \sigma_\beta$  were used to rationalize the three cross-correlation rates listed in Table 1S. As can be seen in Figure 5C, the  $\text{N}-\text{H}^N$  bonds of most residues again appear tilted toward the right ( $\alpha < 0$  in Figure 1). The average value of the  $\alpha$  angles was found to be  $-0.9^\circ$ . This appears to be consistent with valence shell electron pair repulsion (VSEPR) theory, which predicts that the position of the amide proton should be shifted away from the region of higher electron density, which occurs on the left-hand side of the amide nitrogen, toward the region

(25) Kroenke, C. D.; Loria, J. P.; Lee, L. K.; Rance, M.; Palmer, A. G., III. *J. Am. Chem. Soc.* **1998**, *120*, 7905–7915.

(26) Engh, R. A.; Huber, R. *Acta Crystallogr., Sect. A* **1991**, *47*, 392–400.

(27) Tjandra, N.; Feller, S. E.; Pastor, R. W.; Bax, A. *J. Am. Chem. Soc.* **1995**, *117*, 12562–12566.

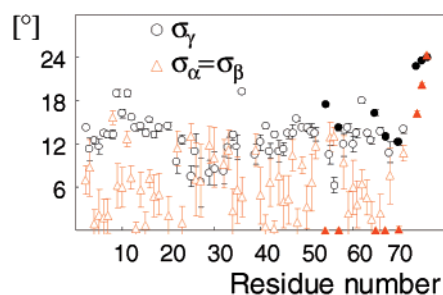


**Figure 6.** Amplitudes of the oscillations in the axially symmetric 3D-GAF model that are parallel (o for  $\sigma_\gamma$ ) and perpendicular ( $\Delta$  for  $\sigma_\alpha = \sigma_\beta$ ) to the  $C^\alpha$ – $C^\alpha$  axis.

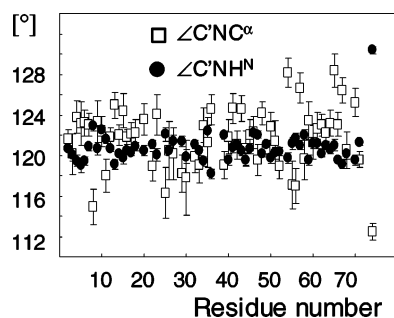


**Figure 7.** Angles  $C'NH^N$  (●) and  $C'NC^\alpha$  (□) from fits of cross-correlated relaxation rates to an axially symmetric 3D-GAF model with  $\sigma_\alpha = \sigma_\beta = 0.5\sigma_\gamma$ .

of lower electron density, on its right-hand side, to minimize electrostatic repulsion.<sup>28</sup> For nonterminal residues the average amplitudes of the oscillations  $\sigma_\gamma$  and  $\sigma_\alpha = \sigma_\beta$  were found to be  $12^\circ$  and  $6^\circ$ , respectively (see Figure 6 and Table 1S). Although we have four rates and four unknowns ( $\alpha$ ,  $\sigma_\gamma$ ,  $\sigma_\alpha = \sigma_\beta$ , and  $\tau_{\text{int}}$ ) the average  $\chi^2$  value was 1. In Figures 5C and 6 all residues with  $\chi^2 > 4$  are represented by filled symbols. A high  $\chi^2$  value could be an indication that the model is not appropriate. However, one has to be very careful in the interpretation, since the rates have been measured with very high precision, so that small structural errors may lead to large (in comparison with the experimental error) deviations of the cross-correlated relaxation rates. There might be small errors in the anisotropic diffusion tensor, the spectra might be polluted by weak impurities, or there might be some undesired coherence-transfer pathways.

The largest source of systematic error in the analysis probably arises from the assumption that the  $C'NC^\alpha$ -angle has a fixed value. Although the average value of  $121.7^\circ$  is well determined by X-ray measurements, it is generally assumed that this angle varies by  $1.8^\circ$  around its average. We have investigated the influence of the  $C'NC^\alpha$ -angle by fitting the experimental rates assuming that  $\sigma_\alpha = \sigma_\beta = 0.5\sigma_\gamma$  and letting this angle free (there are still four fit parameters:  $\alpha$ ,  $\sigma_\gamma$ ,  $C'NC^\alpha$ , and  $\tau_{\text{int}}$ ). In this case all residues could be fitted ( $\chi^2 = 0$  for all residues). In Figure 7 we have plotted the angles  $C'NC^\alpha$  which resulted from the fit. With this motional model we obtain a standard deviation of  $C'NC^\alpha$  of  $2.7^\circ$ . Considering that the average error in this angle resulting from the fit is  $1.6^\circ$  and considering other aforementioned sources of structural errors, this number is remarkably close to the  $1.8^\circ$  standard deviation which is usually assumed in X-ray diffraction. If the  $1.8^\circ$  is not an overestimate

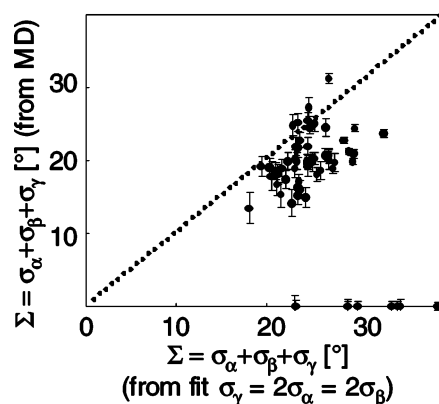


**Figure 8.** Comparison between  $\Sigma = \sigma_\alpha + \sigma_\beta + \sigma_\gamma$  extracted from molecular dynamics simulations and  $\Sigma = \sigma_\alpha + \sigma_\beta + \sigma_\gamma = 2\sigma_\gamma$  obtained from fitting the cross-correlated relaxation rates to an axially symmetric 3D-GAF model with  $\sigma_\gamma = 2\sigma_\beta = 2\sigma_\alpha$ .

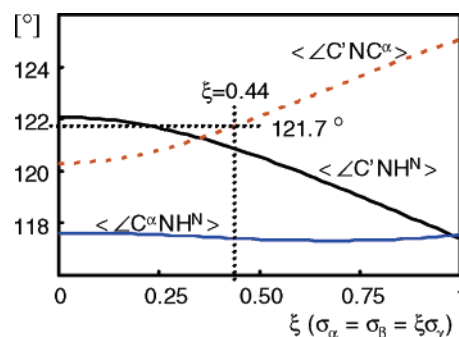


**Figure 9.** Average bond angles around the N nucleus from fits of cross-correlated relaxation rates to an axially symmetric 3D-GAF model with  $\sigma_\alpha = \sigma_\beta = \xi\sigma_\gamma$  as a function of  $\xi$ . The limit  $\xi = 0$  corresponds to the 1D GAF model ( $\sigma_\alpha = \sigma_\beta = 0$ ), while the limit  $\xi = 1$  describes isotropic motion. The canonical angle  $C'NC^\alpha = 121.7 \pm 1.8$  is commonly used in X-ray diffraction studies. This corresponds to  $\xi = 0.44$ .

of the true variation, these results suggest that the internal motions of most residues in ubiquitin can be described by a single model. The motional parameter of this fit has been compared with the molecular dynamics simulations (MD) of Lienin et al.<sup>2</sup> Since only one amplitude ( $\sigma_\gamma$ ) has been fitted in this work, while in the MD simulations the amplitudes of the motions about all three axes have been obtained, it is difficult to determine which parameters to compare. Given that the MD simulations roughly fulfilled the relationship  $\sigma_\alpha = \sigma_\beta = 0.5\sigma_\gamma$ , we decided to compare the sum  $\Sigma = \sigma_\alpha + \sigma_\beta + \sigma_\gamma$  from the MD simulations against  $\Sigma = \sigma_\alpha + \sigma_\beta + \sigma_\gamma = 2\sigma_\gamma$  from our fit of the experimental results. The values from the MD simulations are slightly lower than the ones obtained from our fits, but there is a reasonable overall agreement (see Figure 8). The values with 0 for the MD simulation are residues for which the 3D-GAF model was found not to be valid in the MD simulations.

Finally, we have considered the 3D-GAF model with the  $\sigma_\gamma$  axis parallel to the  $C^\alpha$ – $C^\alpha$  vector and a variable anisotropy parameter  $\xi$  defined by  $\sigma_\alpha = \sigma_\beta = \xi\sigma_\gamma$  ( $\xi = 1$  is equivalent to the isotropic model,  $\xi = 0$  to the 1D-GAF model). In Figure 9, the average bond angles around the N nucleus that resulted from the fits have been plotted as a function of  $\xi$ . With the angle  $C'NC^\alpha$  as a fit parameter, there is no difference in the quality of the fit for different values of  $\xi$ . However, the “X-ray”-value of  $121.7^\circ$  for  $\langle C'NC^\alpha \rangle$  corresponds to a  $\xi$  of 0.44. For the

(28) Atkins, P.; Jones, L. *Chemical Principles*; W. H. Freeman and Company: New York, 2002.

isotropic model ( $\xi = 1$ )  $\langle \angle C'NC^\alpha \rangle = 125.0^\circ$ , while for the 1D-GAF model ( $\xi = 0$ )  $\langle \angle C'NC^\alpha \rangle = 120.3^\circ$ . The average value of  $\alpha$  for  $\xi = 0.44$  is equal to  $-1.7^\circ$ .

In conclusion our results show that the internal motions in ubiquitin are highly anisotropic. When an axially symmetric 3D-GAF model is used the amplitude of the motion about the  $C^\alpha-C^\alpha$  axis is found to be about twice as large as those of the motions about the perpendicular axes. However, the 3D-GAF model might not be the *only* model that can explain our data. The N-H<sup>N</sup> bond was found to be slightly tilted toward the  $C^\alpha$  atom of the same residue.

**Acknowledgment.** This work was supported by the European Union through the Research Training Network "Cross-Correlation" HPRN-CT-2000-00092, by the Fonds National de la Recherche Scientifique (FNRS), by the Commission pour la

Technologie et l'Innovation (CTI) of Switzerland, and by the Centre National de la Recherche Scientifique (CNRS) of France.

**Supporting Information Available:** Experimental schemes for measuring  $R(C'H^N/H^NN)$ ,  $R(NH^N/H^NC^\alpha)$ , and  $R(H^NN/NC')$  cross-correlation rates and their experimental values measured in  $^2D$ -,  $^{15}N$ - and  $^{13}C$ -labeled human ubiquitin. The amplitudes  $\sigma_\gamma$  and  $\sigma_\alpha = \sigma_\beta$  of the axially symmetric 3-D GAF model as well as the angle  $\alpha$  that determines the location of the amide H<sup>N</sup> proton are determined from the rates using an axially symmetric 3-D GAF model. The amplitudes  $\sigma_\gamma = 2\sigma_\alpha = 2\sigma_\beta$  determined from the rates using an axially symmetric 3-D GAF model with the angle  $\angle C'NC^\alpha$  as an additional fit parameter. This material is available free of charge via the Internet at <http://pubs.acs.org>.

JA043575V